Cell, Volume *136*

Supplemental Data

Genetic Interaction of PGE2 and Wnt Signaling Regulates Developmental Specification of Stem Cells and Regeneration

Wolfram Goessling, Trista E. North, Sabine Loewer, Allegra M. Lord, Sang Lee, Cristi L. Stoick-Cooper, Gilbert Weidinger, Mark Puder, George Q. Daley, Randall T. Moon, and Leonard I. Zon

Supplemental Experimental Procedures

Confocal microscopy

TOP:dGFP;*lmo2:DsRed* and *cmyb:GFP*;wnt-modifier outcrosses were heat-shocked and/or exposed to PGE2 modulators as indicated, then subjected to confocal microscopy using a Zeiss LSM confocal microscope (North et al., 2007). Images were acquired in live agarose-embedded embryos, focused on the dorsal aorta and vein within the trunk/tail. AGM cell counts were conducted within a defined 40x region centered on the tip of the yolk sac extension, as indicated in the schematic (>5 embryos/treatment; **Fig.2M**).

FACS analysis

TOP:dGFP; lmo2:DsRed analysis: individual embryos were manually dissociated in 0.9% PBS and examined for GFP and DsRed fluorescence on a BD FACS Calibur.

Adult zebrafish analysis: KM from individual fish was manually dissected in 0.9% PBS at day 3 or 10 post irradiation and examined for alterations in GFP expression or HSC recovery by forward scatter/ side scatter (North et al., 2007).

Murine bone marrow fractionation: WBM was depleted of mature hematopoietic lineages by MACS (Dynal Dynabeads/magnet) and FACS sorted to obtain the cKit+, Sca1+, Lineage- (BD/Pharmingen) fraction as previously described (North et al., 2007).

Murine peripheral blood analysis: blood was obtained at 6, 12, and 24- weeks post-transplant by retroorbital bleed and examined for multilineage contribution >5% by FACS as published previously (North et al., 2007).

qPCR

qPCR was performed on cDNA obtained from whole embryos at 36 hpf (n=20/variable) and individual livers resected from adult zebrafish, using primers listed in Supplementary Table 1. Embryos (n=50) were processed as previously described (North et al., 2007). qPCR (60°C annealing) was performed using SYBR Green Supermix on the iQ5 Multicolor RTPCR Detection System (BioRad), and relative expression levels were determined.

Western blotting

Homogenized zebrafish embryos (12/lane) (Link et al., 2006), murine WBM (50,000 cells lane) and livers were subjected to SDS-PAGE and subsequent Western blotting, using antibodies to β-catenin (1:100, BD), BrdU (1:2000, Sigma), phospho-β-catenin

S675 (1:100, Cell Signaling), phospho-GSK3β S9 (1:100, Cell Signaling), and actin (1:2000, MP Biologicals).

BrdU and TUNEL staining

Zebrafish embryos were exposed to BrdU (10mM)/ 15% DMSO in fish water for 20 mins on ice prior to fixation with PFA. Whole mount processing for BrdU or TUNEL was modified from (Shepard et al., 2005) for 36hpf embryos; staining was detected with HRP-conjugated antibodies and visualized by DAB. Cell counts were performed in the dorsal aorta and vein in 20x fields focused on the tip of the yolk sac extension using Nomarski optics.

Murine colony-forming units-spleen (CFU-S_{12})

WBM cells from the femurs of 8-week old C57Bl/6 or *APC*^{Min} mice, KSL FACS-sorted as described above, were incubated *ex vivo* on ice for one hour with the following individually or in combination as indicated: dmPGE2 (10 μM), indo (10 μM), BIO (0.5 μM), Dkk1 (10 ng/ml), forskolin (1.0 μM), cholera toxin (0.5 μM), EtOH control (n=5/treatment x 2 replicates). Recipient mice were lethally irradiated with a split dose of 10 Gy, and 500 KSL cells were injected retro-orbitally. Spleens were dissected on day 12, weighed and fixed with Bouin's solution; hematopoietic colonies per spleen were counted.

Murine long-term competitive bone marrow repopulation assay

WBM from CD45.1 C57Bl/6 mice was incubated with chemicals ex vivo as described above. Treated-test cells were transplanted into irradiated CD45.2 recipients (n=5/variable x 2) with untreated CD45.1/CD45.2 competitor at the following ratio: 15,000:200,000 (0.075:1). PB was obtained at 6, 12 and 24 weeks post-transplantation, and multilineage reconstitution of the test population determined by FACS as above for each series of treatment populations. Frequency of PB chimerism >5% was used to calculate the total number of chimeric recipients per treatment group. Analysis of APC^{Min} (CD45.2) mice was conducted as described above; CD45.1 mice were utilized as recipients.

Zebrafish fin regeneration

Adult zebrafish were anesthetized and fins were amputated as previously described (Stoick-Cooper et al., 2007). Fish were allowed to regenerate in 20μM indo versus DMSO, and the drug was changed daily. Fins were analyzed after 7 days.

Supplemental Figure Legends

Figure S1

Model of the genetic interaction between wnt and PGE2-signaling pathways in stem and progenitor cell populations during development and regeneration

PGE2-signaling interacts with the wnt/β-catenin pathway at the level of the β-catenin destruction complex and direct modification of β-catenin stability in vivo. This is achieved via G-protein coupled receptor-induced increase in cAMP, resulting in activation of PKA. PKA both phosphorylates β-catenin at S675, resulting in stabilization of the protein by prohibiting ubiquitination, and phosphorylates GSK3β at S9, thereby decreasing its ability to associate with the other members of the β-catenin destruction complex.

Figure S2

PGE2 regulates wnt activity within the HSC/endothelial population

FACS analysis was performed on *TOP:dGFP; lmo2:dsRed* embryos at 36 hpf after exposure to DMSO, 10μM dmPGE2, or 10μM indomethacin. Graphs summarize the relative frequency of cells in the indicated populations. *All differences were statistically significant, ANOVA, $p<0.05$, $n=7$; mean ± SD.

(A) Quantification of cells in the upper half (dsRed+), representing all HSC/endothelial cells; these results confirm the positive effect of and requirement for PGE2 on the total HSC/endothelial cell population.

(B) Quantification of cells in the right half (dsRed+), representing all wnt-active cells; these results confirm the effects of PGE2 signaling on total wnt activity documented in Figure 1.

(C) Quantification of cells in the upper left quadrant (GFP-; dsRed+), representing HSC/endothelial cells without wnt activity.

(D) Quantification of cells in the upper right quadrant (GFP+; dsRed+), representing wnt-active HSC/endothelial cells.

(E) Quantification of cells in the lower right quadrant (GFP+; dsRed-), representing wnt-active cells, excluding the HSC/endothelial population.

Figure S3

PGE2 affects the expression of HSC and vascular markers by increasing β-catenin levels

Embryos were heat shocked at 5 somites and then exposed to DMSO, 10μM dmPGE2, or 10μM indomethacin as indicated from 10 somites until 36 hpf.

(A – E) Quantitative PCR was performed on cDNA obtained from whole embryo extracts. The primers are listed in Supplementary Table 1. An asterisk (*) indicates a statistically significant difference compared to the wild-type control, ANOVA, $p<0.001$, $n\geq5$ sets of 50 embryos/condition; data shown as mean ± SD.

(A and B) wnt and PGE2 pathway modulation affected the expression of HSC markers *runx1* and *cmyb.*

(C and D) wnt and PGE2 pathway modification altered the expression of the vascular marker *flk1* and arterial marker *ephrin B2*.

(E) The wnt target *cyclin D1* was also affected by the interaction of wnt and PGE2 signaling.

(F - J) *wnt8* induction and dmPGE2 treatment synergistic regulated *runx1/cmyb*+ HSCs; exposure of wild-type embryos to dmPGE2 enhanced HSC number **(G)**, as did induction of *wnt8* **(H)**. Combinatorial treatment **(I)** lead to increased *runx1/cmyb* staining in 25/41 embryos. **(J)** In 5/41 embryos, *runx1/cmyb* expression was reduced compared to wild-type after combined treatment with *wnt8* and dmPGE2, indicating a potential negative effect of overactivation of the wnt pathway on HSC formation.

(K) Western blot analysis of total β-catenin in zebrafish embryo homogenates (12 embryos/lane) at 36 hpf. Induction of *wnt8* as well as dmPGE2 treatment increased β-catenin, while indomethacin decreased levels in both wild-type and *wnt8* embryos.

(L) qPCR for β-catenin revealed a lack of transcriptional upregulation following wnt8 induction or dmPGE2 treatment (ANOVA, p=0.937, n=6 sets of 50 embryos/condition).

Figure S4

PGE2-mediated modulation of wnt signaling affects cell death and proliferation

(A – D) Indo treatment enhanced TUNEL+ cells in the AGM in both WT and *wnt8* induced embryos; median representatives are shown.

(E – L) Induction of *dkk*, *axin*, or *dnTCF* enhanced apoptosis; dmPGE2 improved this effect only in *dkk* transgenics.

(M – P) Induction of *wnt8* enhanced BrdU incorporation, while indo treatment diminished BrdU in both WT and *wnt8* embryos.

(Q – X) Inhibition of wnt signaling by *dkk*, *axin*, or *dnTCF* diminished BrdU incorporation; the effect of *dkk* could be rescued by dmPGE2.

Figure S5

PGE2 enhances wnt activity in the HSC compartment via the PKA/cAMP pathway

(A – D, F - K) *In situ* hybridization for *GFP* in *TOP:dGFP* wnt reporter embryos following treatment with modifiers of PGE2/cAMP/PKA-mediated signaling at 36 hpf.

(A and C) cAMP stimulation by forskolin (0.5μM) enhanced the number of wnt active cells within the tail region of the zebrafish embryo.

(B and D) Indomethacin (10μM) decreased wnt activity in the zebrafish embryo. This effect could be rescued by the addition of forskolin.

(E) Quantitative summary of the effects of indomethacin and forskolin on *TOP:dGFP*+ cells in the AGM region. * statistically significant between each other, ANOVA, p<-0.001, n=10).

(F and G) Exposure to dmPGE2 enhanced *GFP* expression in the tail region.

(H and I) PKA inhibition by H89 (0.5μM) decreased wnt activity in wild-type embryos and diminished the wnt-enhancing effects of dmPGE2.

(J and K) Inhibition of PI3K by LY294002 (1μM) had no effect on wnt activity in wild-type and dmPGE2-treated embryos.

(L) Summary of the effects of dmPGE2, H89, and LY294002 on *TOP:dGFP*+ cells in the AGM region. * statistically significant between each other, ANOVA, p<0.001, n=10).

Figure S6

PGE2 enhances wnt activity in the HSC compartment via the PKA/cAMP pathway

(A and B) qPCR results for *runx1* expression after *wnt8* transgene induction and chemical treatments. * statistically significant vs. control; ** statistically significant vs. *wnt8* (**A**) or dmPGE2 (**B**), ANOVA, $p<0.001$; n=3 sets of 50 embryos; data represented as mean ± SD.

(A) cAMP stimulation by forskolin (0.5μM) and *wnt8* induction enhanced *runx1* levels at 36 hpf in qPCR analysis of whole embryo lysates. Forskolin improved the negative effects of indomethacin treatment in both controls and *wnt8* transgenics.

(B) PKA inhibition by H89 (0.5μM) reduced *runx1* expression by qPCR in both control and dmPGE2 treated embryos.

(**C and D**) dmPGE2 (10μM) enhanced *runx1/cmyb* expression in the zebrafish tail at 36 hpf.

(**E and F**) PKA inhibition by KT5720 (1μM) had similar effects on HSC number in wild-type and dmPGE2-treated embryos as seen with H89 exposure.

(**G and H**) PI3K inhibition by LY294002 (1μM) or (**I and J**) Wortmannin (1μM) did not affect HSC number in wild-type or dmPGE2-treated embryos.

Figure S7

The PGE2/wnt interaction affects hematopoietic colony formation in murine ES cells

(**A and B**) ES cell hematopoietic colony formation assays were performed; cells were exposed to soluble modulators of the wnt pathway (10 ng/ml Wnt3A of 400 ng/ml Dkk1)

and then incubated with indomethacin (20 μM), dmPGE2 (10μM), or forskolin (5 μM) as indicated. Colony forming units-Culture (CFU-E (erythroid), CFU-M (monocyte), CFU-G (granulocyte), CFU-GM (granulocyte-monocyte), and CFU-GEMM (granulocyte-erythroid-monocyte-megakaryocyte)) were scored on day 8-10 based on morphology. Averages +/-SEM in the fold changes in total CFU-C number of each sample relative to control were calculated from at least six individual experiments.

(**A**) The positive effect of wnt activation on hematopoietic differentiation could be diminished by inhibition of prostaglandin synthesis with indomethacin. Wnt3A enhanced hematopoietic colony formation. Indomethacin (20μM) alone diminished colony number and inhibited the enhancing effects of Wnt3A (* statistically significant vs. control, t-test, $p=0.002$, ** statistically significant vs. indomethacin, $p<0.001$; $n=6$).

(B) Inhibition of wnt activity decreased hematopoietic differentiation and could be rescued by PGE2 or cAMP signaling. Inhibition of wnt activation by Dkk1 (10ng/ml) diminished colony number. dmPGE2 (10μM) and the cAMP activator forskolin (0.5μM) enhanced hematopoietic colonies. This negative effect of Dkk1 could be rescued by both dmPGE2 or forskolin, confirming the role of PKA in this process. (* statistically significant vs. control, t-test, $p=0.005$, *** statistically significant vs. Dkk1, $p<0.046$; $n=4$).

(C) Western blot analysis of ES cell lysates. Wnt3A and dmPGE2 treatment enhanced β-catenin levels, while indomethacin and Dkk1 had negative effects. Indomethacin diminished the enhancing effect of Wnt3A, whild dmPGE2 could enhance β-catenin levels after Dkk1 exposure.

Figure S8

PGE2 affects hematopoietic progenitor function by enhanced cAMP production and subsequent phosphorylation events

(A – B) CFU-S_{12} colony formation after transplantation of 500 purified KSL cells into irradiated recipient C57Bl/6 mice. Spleens were dissected at day 12 after transplantation and colonies counted.

(A) Effect of *in vivo* treatment of lethally irradiated recipient mice with indomethacin (2.5 mg/kg, i.p., q.o.d.), BIO (50μg/kg), or both, on CFU-S_{12} colony formation; BIO treatment significantly increased colony formation, which could be inhibited by concurrent treatment with indomethacin (* statistically different from control and other treatments, t-test, $p=0.015$, $n\geq7$).

(B) Effect of *ex vivo* treatment of purified KSL cells with Dkk1 (10ng/ml), dmPGE2 (10μM), forskolin (Fors; 1μM), cholera toxin (Chol Tox; 0.5μM) and/or a combination of drugs as indicated on $CFUS_{12}$ activity. Inhibition of wnt activity by Dkk1 reduced colony formation. This effect could be rescued by both dmPGE2 and direct cAMP stimulation by forskolin or cholera toxin; * statistically significant vs. control, ANOVA, $p<0.05$, n=7-10.

(C) cAMP luminescence assay in isolated murine bone marrow cells; luminescence intensity is inversely related to cAMP levels. Exposure of bone marrow with dmPGE2 and forskolin for 15 minutes had dose-dependent enhancing effects on cAMP levels (mean ± SD, n=3).

(D) Western blot analysis of homogenized murine bone marrow cells following *ex vivo* drug treatment. Total β-catenin levels increased in a time-dependent fashion following

exposure to dmPGE2 (10μM), and decreased in response to indomethacin (10μM). The response of phospho-β-catenin(S675) and phospho-GSKβ(S9) to drug treatment was also time dependent, and preceded effects on total β-catenin.

Figure S9

The interaction of PGE2 and wnt affects regeneration in several organs

(A - H) Immunohistochemical analysis of liver samples 1 day post 2/3 partial hepatectomy in C57Bl/6 and *APC*^{Min} mice. Photomicrographs were taken at 20x magnification.

(A and E) Heterozygous *APC* loss enhanced site-specific phosphorylation of β-catenin (S675) post liver resection.

(B and F) Heterozygous *APC* loss enhanced site-specific phosphorylation of phospho-GSK3β (S9).

(C, D, G, H) Inhibition of prostaglandin synthesis with indomethacin (2.5 mg/kg twice daily intraperitoneal injections) resulted in undetectable levels of phospho-β-catenin (S675) and phospho-GSK3β (S9).

(I) Inhibition of PGE2 production by indomethacin diminished total β-catenin levels and site-specific phosphorylation of β-catenin (S675) and GSK3β (S9) in mice following partial hepatectomy by western blot analysis.

(J) Inhibition of PGE2 synthesis increased hepatocellular necrosis in regenerating mouse livers. Histological sections of mouse livers were examined for extensive areas of necrosis. Sections with more than 4 areas of necrosis were counted as positive. Indomethacin increased areas of necrosis in wild-type and APC^{Min} mice.

(K and L) Effect of PGE2 inhibition on zebrafish fin regeneration.

(K) Following amputation, the zebrafish caudal fin regenerated completely over 7 days through a wnt-mediated process of progenitor proliferation (blastema).

(L) Treatment with indomethacin (20μM) completely blocked the regenerative process compared with DMSO-treated controls (n=3/3).

Table S1

PCR primer sequences

beta actin F	5’-GCTGTTTTCCCCTCCATTGTT
beta actin R	5’-TCCCATGCCAACCATCACT
eGFP F	5’-CTGGTCTAGCTGGACGGCGACG
eGFP R	5’-CACGAACTCCAGCAGGACCATG
runx1 F	5’-CGTCTTCACAAACCCTCCTCAA
runx1 R	5’-GCTTTACTGCTTCATCCGGCT
cmyb F	5’-TGATGCTTCCCAACACAGAG
cmyb R	5’-TTCAGAGGGAATCGTCTGCT
flk1 F	5’-CGAACGTGAAGTGACATACGG
flk1 R	5’-CCCTCTACCAAACCATGTGAAA
cyclinD1 F	5’-GGAACTGCTGGCGCTTAAATA
cyclinD1 R	5’-GACTTGCGAGAGGAAGTTGG
ephrin B2 F	5’-CAAGGACAGCAAATCGAATG
ephrin B2 R	5’-TGAGCCAATGACTGATGAGG

Supplemental References

Link, V., Shevchenko, A., and Heisenberg, C.P. (2006). Proteomics of early zebrafish embryos. BMC Dev Biol *6*, 1.

North, T.E., Goessling, W., Walkley, C.R., Lengerke, C., Kopani, K.R., Lord, A.M., Weber, G.J., Bowman, T.V., Jang, I.H., Grosser, T.*, et al.* (2007). Prostaglandin E2 regulates vertebrate haematopoietic stem cell homeostasis. Nature *447*, 1007-1011.

Shepard, J.L., Amatruda, J.F., Stern, H.M., Subramanian, A., Finkelstein, D., Ziai, J., Finley, K.R., Pfaff, K.L., Hersey, C., Zhou, Y., *et al.* (2005). A zebrafish bmyb mutation causes genome instability and increased cancer susceptibility. Proc Natl Acad Sci U S A *102*, 13194-13199.

Stoick-Cooper, C.L., Weidinger, G., Riehle, K.J., Hubbert, C., Major, M.B., Fausto, N., and Moon, R.T. (2007). Distinct Wnt signaling pathways have opposing roles in appendage regeneration. Development *134*, 479-489.

Supplemental Figure 1.

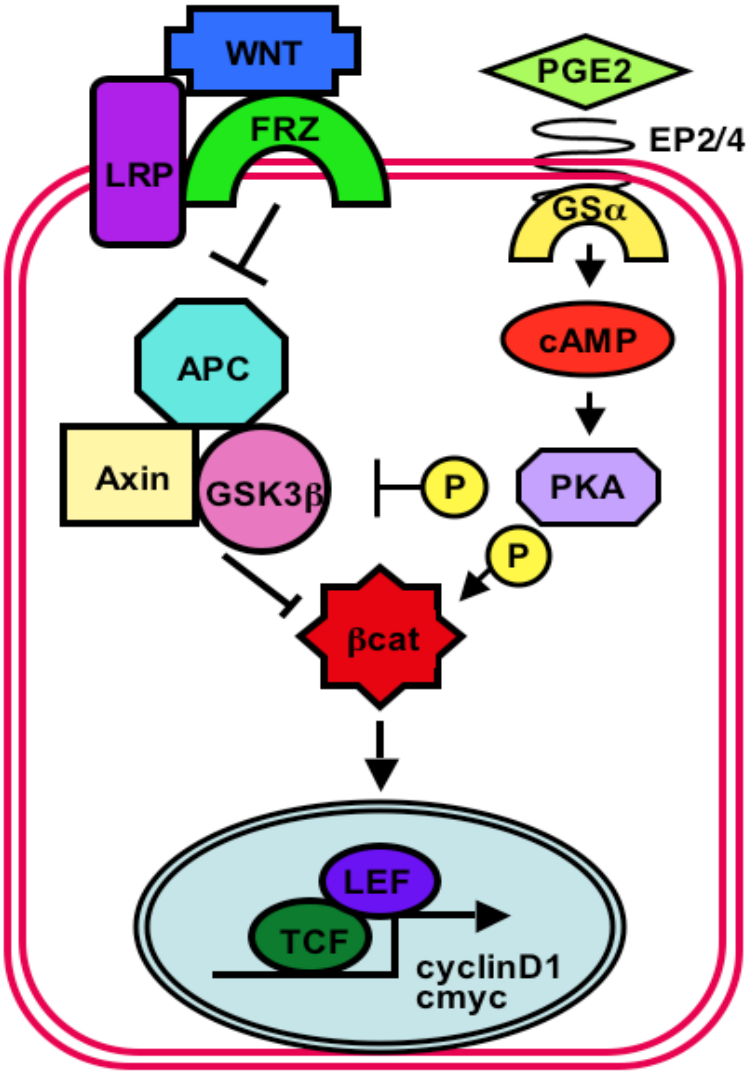

Supplemental Figure 2.

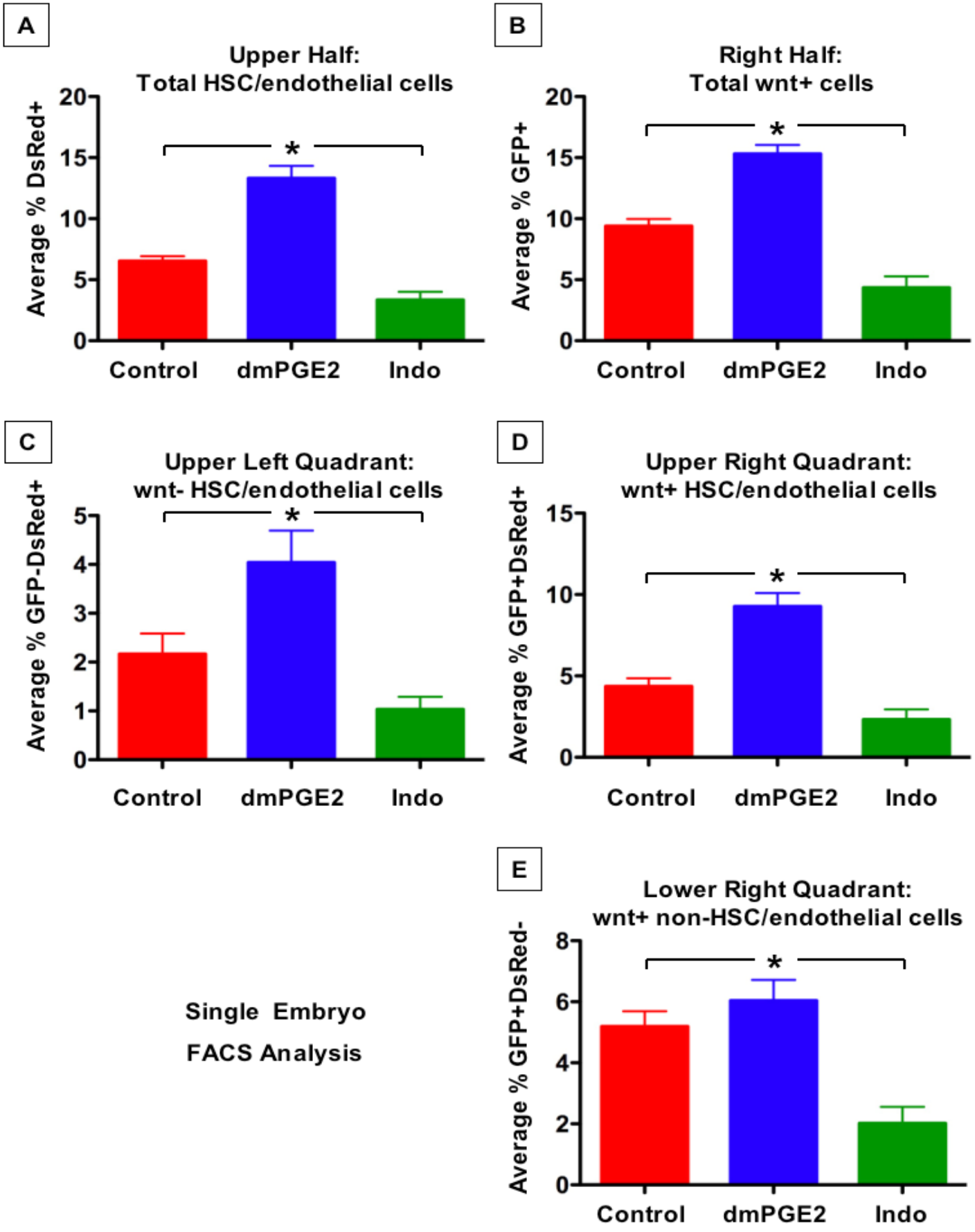

Single Embryo

FACS Analysis

Supplemental Figure 3.

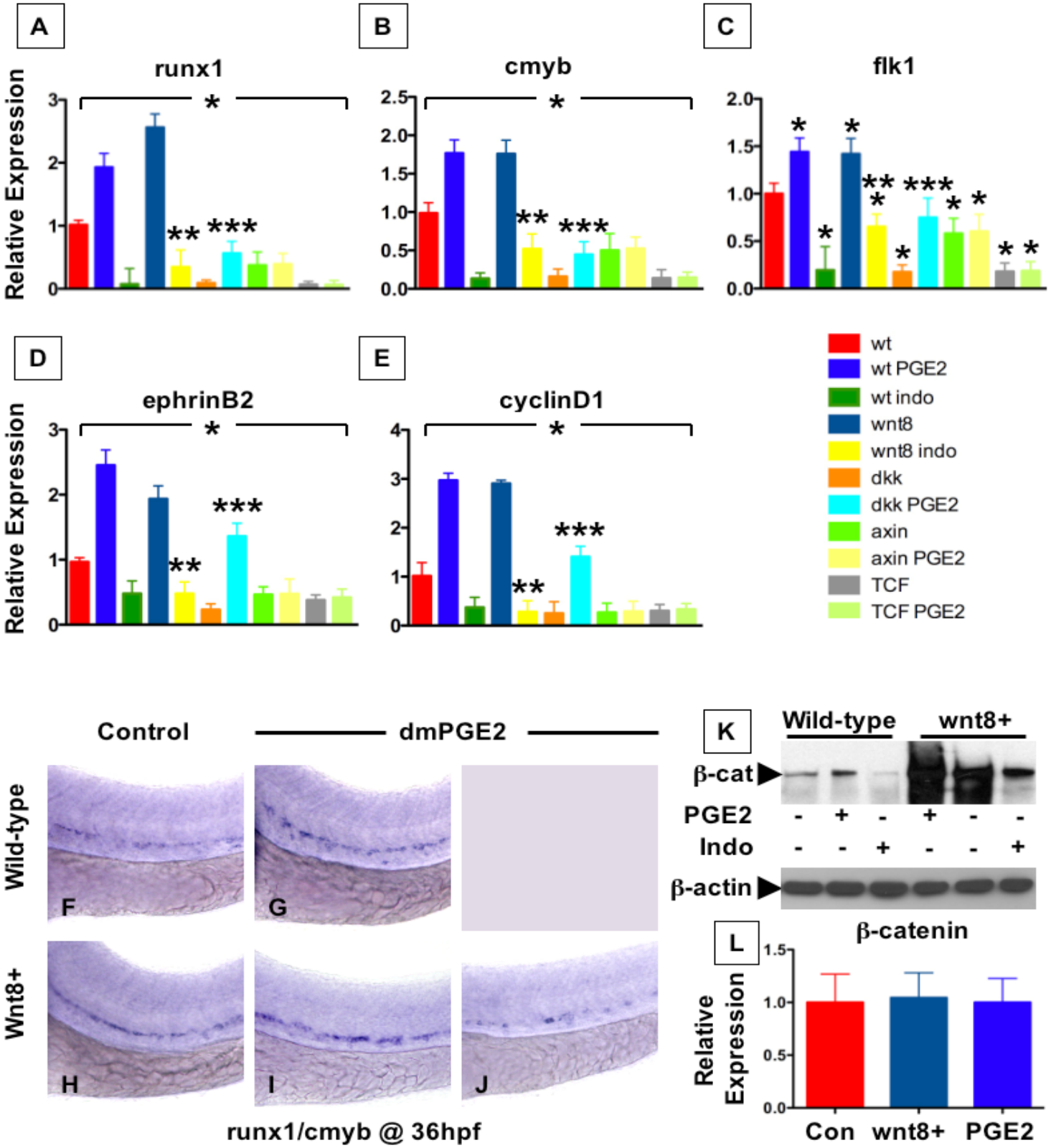

Supplemental Figure 4.

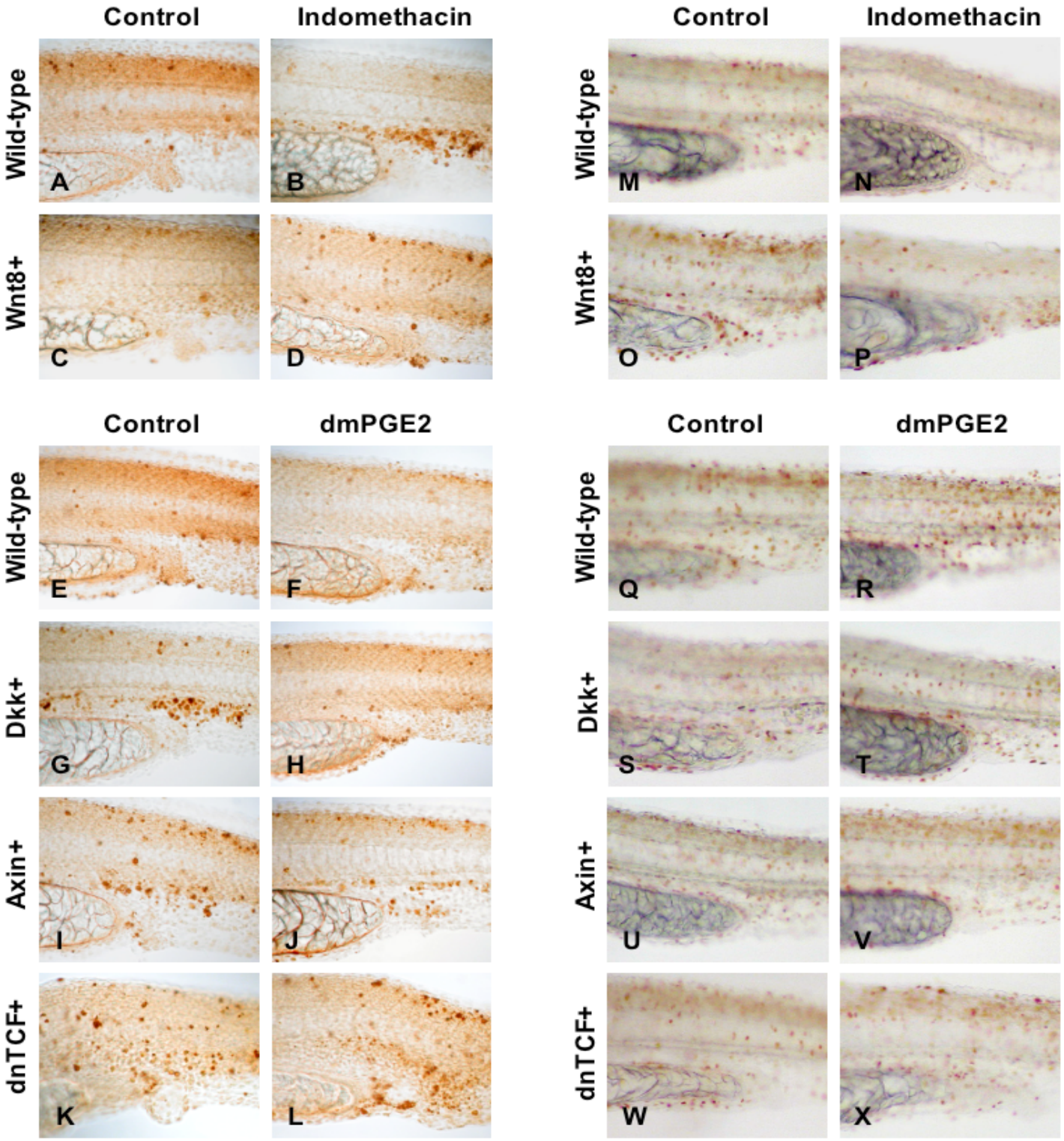

Supplemental Figure 5.

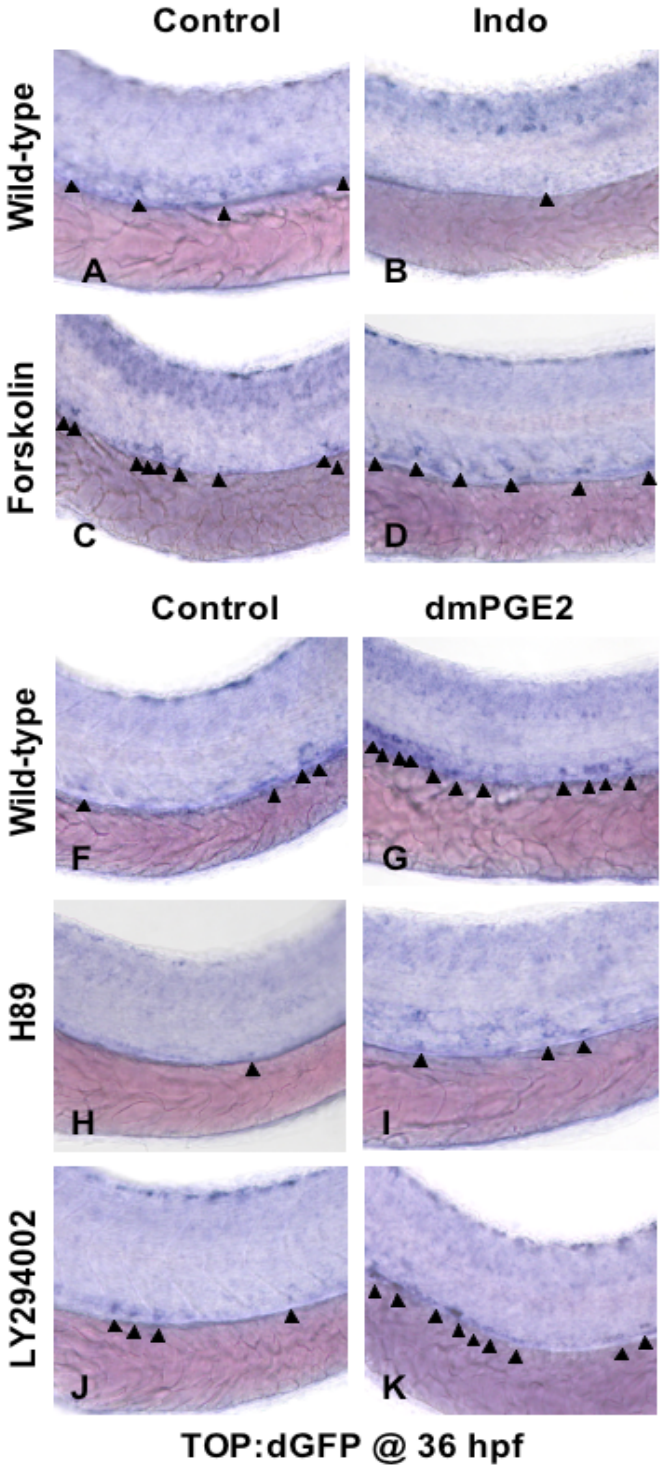

TOP:dGFP @ 36 hpf

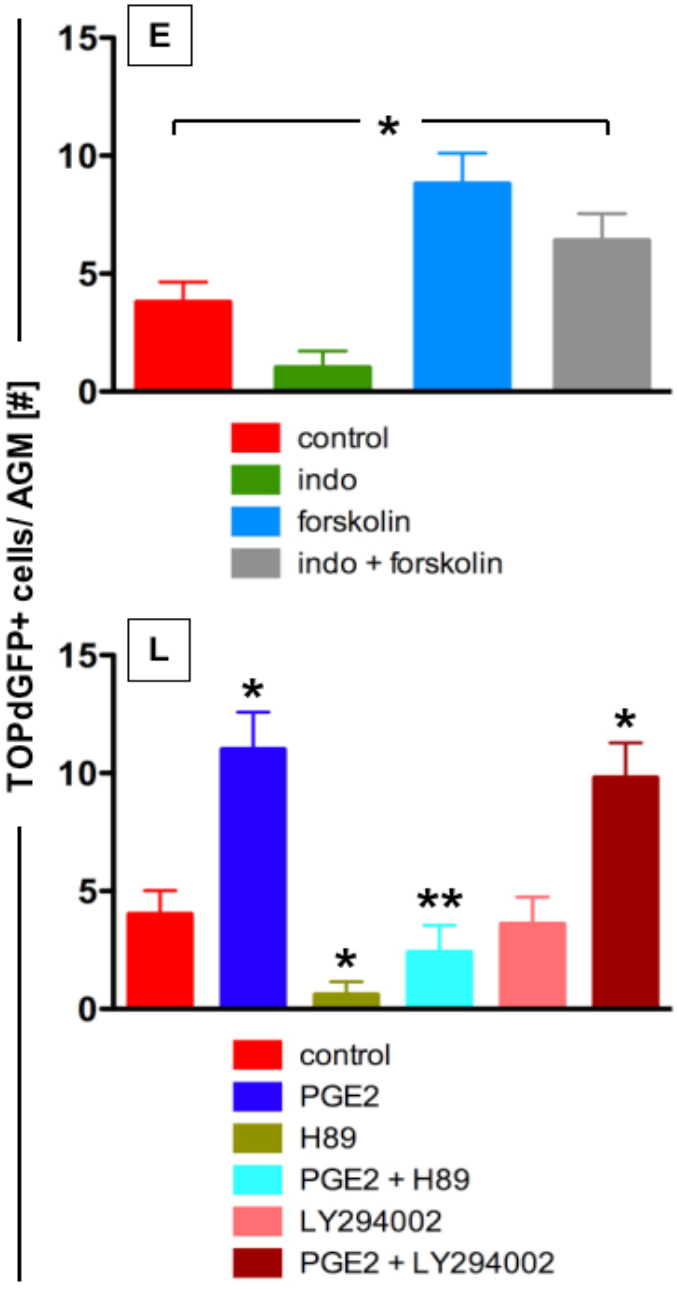

Supplemental Figure 6.

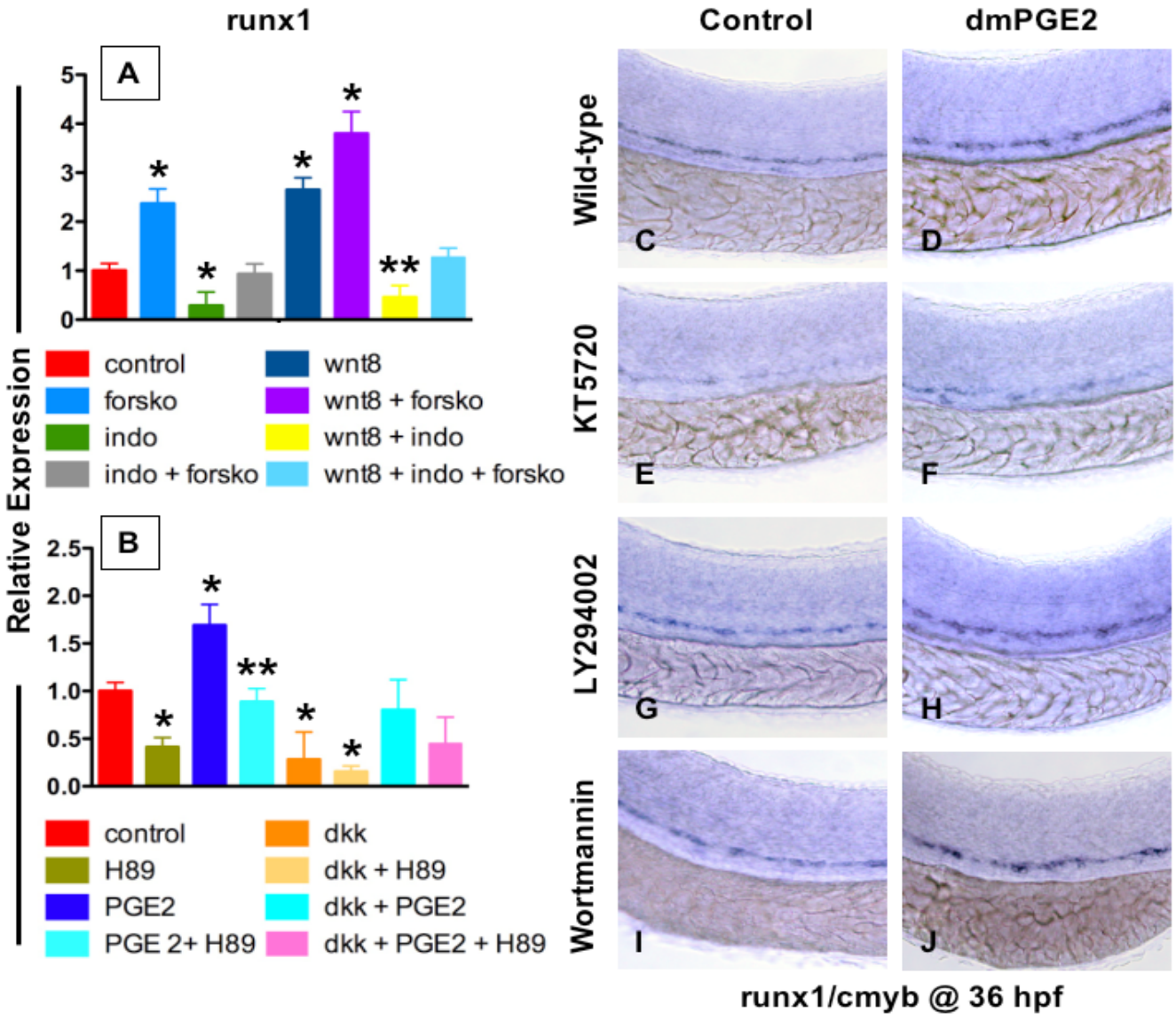

Supplemental Figure 7.

A

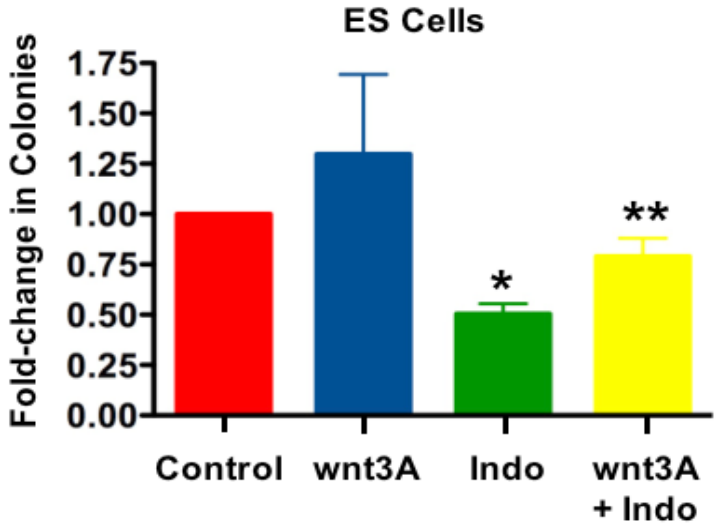

B

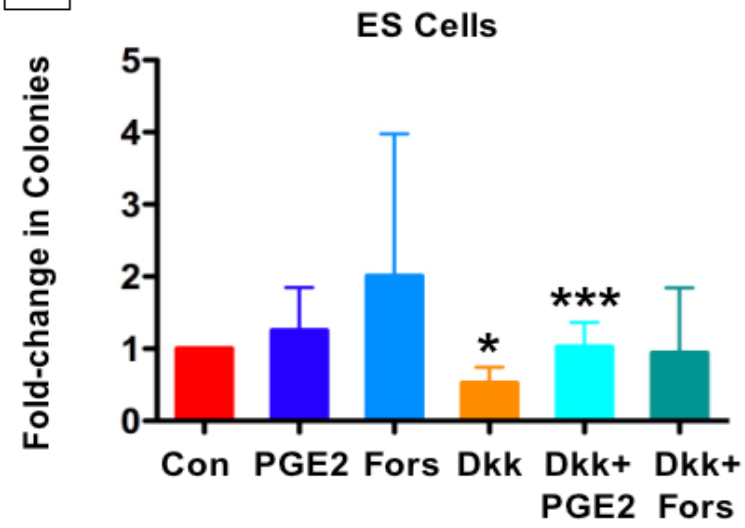

C

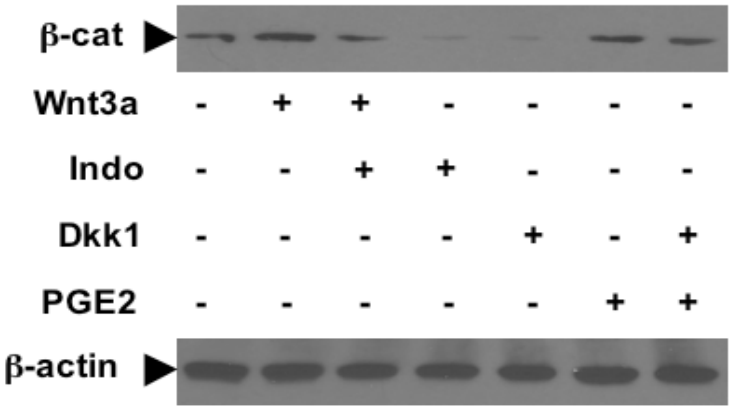

Supplemental Figure 8.

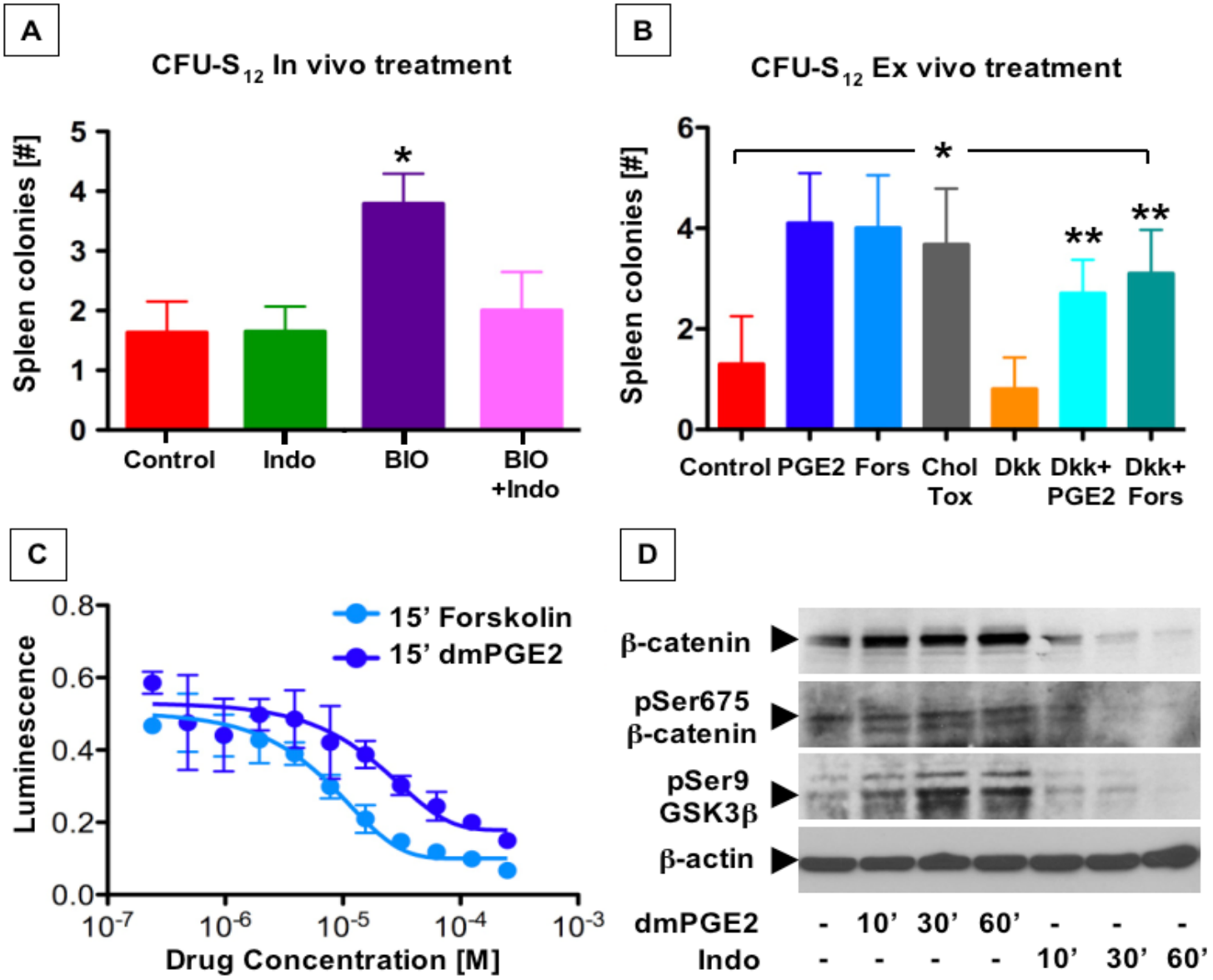

Supplemental Figure 9.